Journal of Astronomical Telescopes, Instruments, and Systems

AstronomicalTelescopes.SPIEDigitalLibrary.org

Review on thermal and mechanical challenges in the development of deployable space optics

Víctor Villalba
Hans Kuiper
Eberhard Gill

SPIE.

Víctor Villalba, Hans Kuiper, Eberhard Gill, "Review on thermal and mechanical challenges in the development of deployable space optics," *J. Astron. Telesc. Instrum. Syst.* **6**(1), 010902 (2020), doi: 10.1117/1.JATIS.6.1.010902

REVIEW

Review on thermal and mechanical challenges in the development of deployable space optics

Víctor Villalba,* Hans Kuiper, and Eberhard Gill
Delft University of Technology, Department of Space Engineering,
Faculty of Aerospace Engineering, Delft, The Netherlands

Abstract. Deployable optics promise a revolution in the capability of observing the universe by delivering drastically reduced mass and volume needs for a desired level of performance compared to their conventional counterparts. However, this places new demands on the mechanical and thermal designs of new telescopes, essentially trading mass and volume for structural and control complexity. We compile the thermomechanical challenges that should be taken into consideration when designing optical space systems, as well as summarize 14 projects proposed to address them. Stringent deployment repeatability requirements demand low hysteresis, whereas stability requirements require high stiffness, proper thermal management, and active optics. © *2020 Society of Photo-Optical Instrumentation Engineers (SPIE)* [DOI: 10.1117/1.JATIS.6.1.010902]

Keywords: deployable optics; deployment mechanisms; microdynamics; athermalization; vibration.

Paper 19088V received Aug. 28, 2019; accepted for publication Feb. 19, 2020; published online Mar. 13, 2020.

1 Introduction

The maximum achievable resolution, for a given distance to the object and wavelength, of an optical system is determined by the physical aperture of its entrance pupil. Therefore, a telescope intended to observe distant targets with high detail needs a large aperture. In addition, a long focal length allows larger demagnification of the object.

Deployable space optical instruments originally gathered attention within the astronomical community due to their potential to increase the primary aperture and the focal length of space telescopes beyond the limits imposed by launch vehicle fairings. The precursor technology to these systems is the use of segmented aperture mirrors in ground-based observatories.[1] In these systems, manufacturing capabilities and gravity sag impose limits to the achievable size of individual mirrors.[2] The engineering effort to produce a deployable space telescope (DST) with a segmented aperture has crystallized in the James Webb Space Telescope (JWST), an optical to infrared (IR) astronomical telescope to be launched into an L2 orbit in 2021.[3]

At the same time, the Earth Observation (EO) market has experienced consistent growth over the past decade, with very high resolution (VHR) imaging, defined as ground sampling distances (GSDs) of less than 1 m, taking the larger piece of the total market value. The sector was estimated to be worth $1.6 billion in 2014, with current projections predicting a total value of $8.5 billion worldwide by 2026.[4]

From a typical low Earth orbit (LEO), primary mirror apertures in VHR systems such as Worldview 4 are in the order of 1 m.[5] While it is possible to fit such a system in a conventional launcher fairing, the resulting systems with conventional, rigid configurations are very heavy. The state-of-the-art Worldview-3 satellite weighs 2800 kg.

Here deployable space optics have also attracted a lot of attention in recent years due to their ability to enable cheaper and more agile deployment of large aperture systems, which also increases the possible GSD and therefore the market value of the observations. The fact that large apertures can be folded and "stowed" in the launcher occupying a fraction of their total size makes it possible to have much larger resolutions without the need of heavy launchers.

*Address all correspondence to Víctor Villalba, E-mail: v.m.villalbacorbacho@tudelft.nl

In addition, there are possibilities for multiple deployments and piggybacking as a strategy to further reduce launch cost.[6]

This paper is the result of the literature study performed as part of the TU Delft (TUD) DST[7] with the purpose to guide development of its structure and deployment mechanisms. This is a proposal for a VHR EO telescope, but the findings reported herein are valid for other mission profiles and architecture.

The objective of this paper is to analyze the structural peculiarities that make deployable space optics particularly challenging compared to their monolithic predecessors and also to provide a review of how different proposals have addressed some of these challenges. This will then lead to some conclusions regarding current technological challenges, a rationale to solve them, and the maturity of the different projects that are examined. While complete instruments have more subsystems, this paper refers only to the mechanical development of the optical telescope elements (OTEs), which do not include additional optical systems and detectors. However, other elements, such as baffles and sunshields, will also be discussed due to their importance for the stability of OTEs.

This paper is organized as follows: first, a review of the thermomechanical challenges that deployable space optics need to overcome is presented. Then, the deployable optics projects reported in the literature are summarized, with special attention to their thermal and mechanical issues. Finally, conclusions are drawn regarding the technological advances, which enable deployable optics systems.

2 Thermomechanical Challenges in Deployable Space Optics

Edeson et al.[8] provided a review of typical threats to dimensional stability of conventional space optics. The authors of that paper refer to conventional optics as opposed to systems with active correction of degrees of freedom (DOFs). These threats apply to deployable optics as well. The authors exposed the physical causes of instability in general and went on to analyze the characteristics of the materials and joints used for ultrastable structures. Finally, the authors described the analysis and testing procedures used to validate and verify these structures. The general flow of information in the paper by Edeson et al. can be seen in Fig. 1.

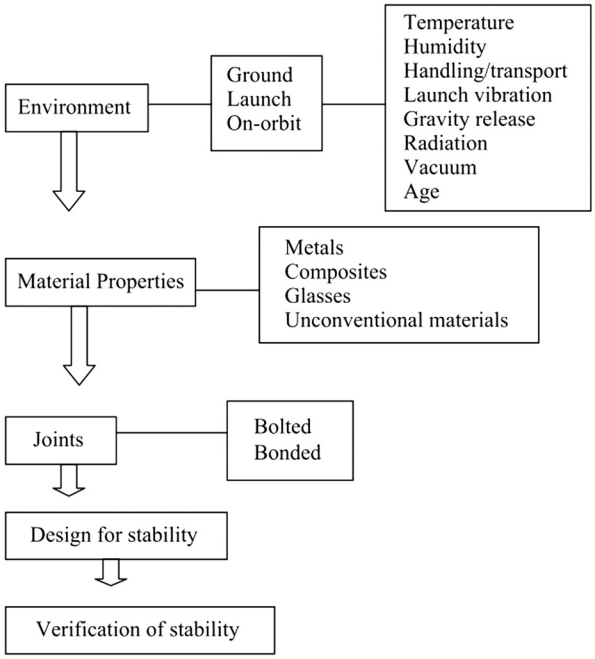

Fig. 1 Summary chart of a review on dimensional stability of space optics.[8]

This section is intended to add to the description of those issues in the case of deployable optics and include some that are specific to the new structures. Deployable telescopes, compared to typical space optics, have more deployment mechanisms with more stringent misalignment budgets, which are sources of microdynamic instability. They also have longer structures only supported at their base, which means they tend to be less stiff, aggravating dynamic issues. In addition, those support structures have small thermal mass and are more exposed to external heat fluxes due to the difficulty of adding shielding or insulation. These characteristics give rise to issues in "microdynamics" and thermal flutter, as well as aggravate classic problems such as the need for gravity offloading.

2.1 *Impacts of Atmospheric Conditions*

The first stage in the life of an instrument once it has been manufactured involved testing and storage on the ground. The structure of the telescope will need to be kept in conditions that mimic those encountered in space for alignment critical operations. Therefore, stability to variable ground conditions is beneficial. In addition to the standards of cleanliness inherent to any space instrument, there is the need to control for two more effects: temperature and humidity.

Thermal distortion is one of the operational challenges, which will be discussed later in this paper with more detail, though of course there is the need to maintain the stability of the test setup during alignment tests. The effect of thermal creep, particularly in materials with polymeric matrices, such as the common place carbon fiber-reinforced plastics (CFRP), also needs to be taken into consideration, as heavy structures under permanent load can creep out of specifications if the storage temperature is high enough. Depending on the material, a significant fraction of this creep may be recovered,[9] but it still poses a danger to the structure's repeatability.

Hygral expansion is also an important issue since any humidity absorbed by the materials will tend to outgass in space, eliminating the swelling of the structure on the ground. This is not a major concern for metallic or ceramic materials, or for their composites, but it can have an effect on materials with a polymeric base.[10,11] Most assembly operations are carried out in humid air, so the components need to be coated with a moisture barrier to prevent excessive absorption. A system that is sensitive to moisture will need to receive a "bakeout" treatment, which removes this expansion prior to operations on the ground. Another mitigation technique is to store the critical components in a dry atmosphere and only getting them out for short periods for alignment operations. Note that performing a bakeout prior to alignment may be good practice, but if the structure is allowed to swell before launch, the absorbed moisture may deposit in other surfaces of the spacecraft, compromising other subsystems.

2.2 *Gravity Release and Testing Procedures*

Regarding their structural integrity, space structures in general can be considered to experience nearly no loads, with the notable exception of thermal loads due to temperature gradients. In deployable structures, the deployed configuration is not necessarily designed to support its own weight on Earth.[12,13] This forces the testing phase to use gravity offloading procedures to simulate deployment procedures and deployed-state performance. This is typically achieved by hanging the structure from several points that can move without friction parallel to the direction of the motion but compensate gravity or supporting it with rollers on the floor.

This is true of most deployable structures, such as antennas and solar panel assemblies. Optical structures are different since they have stringent three-dimensional precision deployment requirements. Therefore, it is important that the gravity offload system does not overconstrain the motion of the structure. This is difficult to achieve, because gravity, being a distributed force, creates stresses within a structure supported from discrete points, which can be mitigated by adding more support points, thereby negating the principle of exact constraint. Ideally, such a system would have zero stiffness in the vertical direction, which is an emerging property of certain structural configurations. A general description of zero-stiffness mechanisms is given by Schenk and Guest.[14] Another possibility is to use a pressure-controlled flow to provide stable force output.[15]

There is an additional issue when testing the optical systems because large aperture mirrors also need to withstand their own weight during ground testing. Mirror materials, usually technical ceramics such as silicon carbide or metals, are very stiff, but the allowable surface figure error requirements during testing may pose a significant engineering challenge due to the need for special large mounts and cranes to move them around or test their performance.[16] This is an old problem and not exclusive to deployable telescopes. One of the mitigation strategies is using simulations with different mounting boundary conditions, and extracting the zero-gravity sag from the deflections resulting from pointing the mirror upward and downward.[17]

2.3 *Launch and Deployment Failures*

Launch is the most structurally challenging event faced by the spacecraft, with the possible exceptions of in-orbit collision or re-entry. Loads experienced during transportation and handling may also be an issue with large space structures in general.[18] Development of space structures capable of withstanding these loads is a wide topic and covering it is well beyond the scope of this paper. An introduction to the subject was written by Wijker.[19] Launch vehicle manufacturers typically present four main profiles to describe the mechanical environment within the launcher: static acceleration profile, separation shock response spectrum defined in the payload adapter, sine-equivalent vibration, and acoustic vibration.[20–22] These are standard loads used in the verification procedures for all spacecraft. Loads experienced during transportation and handling may also be an issue with large space structures in general,[18] and they must be included in the analyses.

Like other deployable elements, deployable optics are built so that the stowed state is much stiffer and stronger than the deployed configuration. Going by eigenfrequency as a criterion, launch loads typically require first eigenfrequencies in the order of 100 Hz for the structure to survive, but deployed structures typically have first bending eigenfrequencies below 1 Hz. This imposes the need for hold down and release mechanisms and alternative load paths, which spare the optical elements from excessive loads. Structures typically fail due to yielding or rupture of its components, but it is advisable to keep in mind that microplasticity[8,23] effects can appear well below the nominal yield stress of materials.

2.4 *Microdynamics*

Microdynamics is a term referring to a number of loosely related phenomena, all of which take place below the microscale threshold. In this paper, the term refers to the effects of friction in joints from a purely mechanical source. Other effects that are referred to as microdynamics by other authors, such as thermal snapping, creep, and microyielding are covered in other sections of this paper.[24] This separation is adopted to clarify the causes for each phenomenon, but even in this case, several microscale effects are comprised in this definition. These different effects are difficult to uncouple and observe independently in experiments, and even the terminology in the literature is neither clear nor consistent about it. An effort in this regard was presented by White and Levine,[25] who proposed a framework for the analysis of microdynamic effects. The scope of their definition of microdynamics is the same as in this work.

Microdynamics is also related to structural nonlinearity. Joints are known to present three essential kinds of nonlinearities in their behavior, namely freeplay, nonlinear elasticity, and hysteresis. These effects are illustrated in Fig. 2. These deviations from the ideally linear response

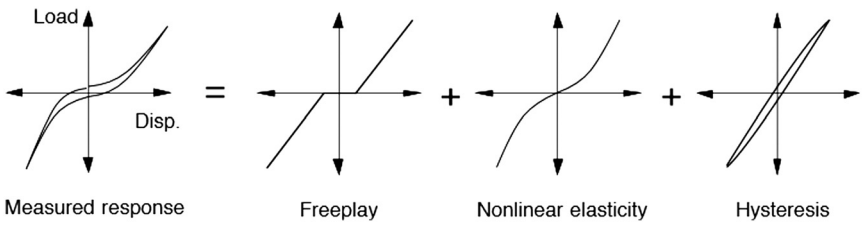

Fig. 2 Three types of nonlinear behavior in mechanical joints.[26]

are known to lower the eigenfrequencies of the structure with respect to a linear approximation, making them significantly less stable against vibration inputs.[27]

The microdynamics of deployable trusses has been the focus of an intense research effort in the context of developing highly stable trusses, such as the one present in NuSTAR.[28] This type of joint-dominated structures experience sudden vibrations during operation, which are consistent with the sudden release of energy previously lost as a result of hysteresis.[29] This is very similar to the phenomenon of thermal snapping but can happen without the influence of a thermal load.[30] Peterson and Hinkle[24] also provide a rationale to lay out hysteresis requirements on large structures. For a given level of acceptable displacement, a stiffer structure is able to accommodate more hysteretic loss with acceptable stability.

The joints where these hysteretic losses occur usually rely on contact surfaces for the transmission of the deployment torque. An example of such mechanism is the ball-bearing hinge developed as part of the Origins program and presented by Lake et al.[31] This was a joint designed to minimize nonlinear responses.

Ingham and Crawley[27] investigated the modal behavior of another deployable truss structure. Very small strains, below 1 $\mu\epsilon$, were shown not to affect the modal shapes of the structure, therefore respecting its linear behavior. Strains above this level, however, did induce a shift in the eigenfrequency and an increase in the observed damping ratio. The researchers conclude that the nonlinear structural damping mechanisms in the joints do not activate for strains below this boundary. An effort to incorporate similar effects was reported by Coppolino et al.,[32] including nonlinearity, stiffness uncertainty, and snapping in joints. The authors created a toolbox to define properties at component level and simulate whole structures in the 100- to 500-Hz frequency band.

Another effect within the microdynamics classification is the so-called microlurching, described by Warren et al.,[33] who found that joint-dominated structures subjected to transient disturbances consistently "lurch" to a new static position once the vibration dissipates. Repeating this event a sufficient number of times makes the structure reach an "equilibrium zone," which was found to be extremely repeatable. This behavior allows positioning a large deployable structure with very high repeatability by using intentional, transient disturbances. The underlying cause of this behavior is understood to be the progressive release of residual strain energy stored at the frictional interfaces prior to the intentional excitation.

2.5 *Microvibration*

Microvibration, also referred to as jitter in the literature when it affects spacecraft attitude, is the presence of small oscillations propagating through the spacecraft structure. In most cases, these vibrations pose no threat to the survival of the said structure, but they can alter pointing of the system and cause misalignment of optical components, in which case it is referred to as wavefront error (WFE) jitter.[34] In fact, this type of vibration is widely considered one of the largest threats to the pointing stability of optical payloads.[35–37]

Reaction wheel assemblies are generally the largest source of vibration in most systems.[36,38] The dynamics of this phenomenon are usually modeled with an unbalanced rotor model with the first harmonic appearing at the reaction wheel speed. Subsequent harmonics, which may be of similar importance, appear as a result of other imperfections in the wheel assembly. Examples of these defects are inhomogeneity of the wheel's mass, worn or irregularly shaped bearings, stick-slip behavior, or freeplay. One may argue that friction effects are also similar or even the same as those described as microdynamics in this text, but for the purposes of this paper, the reaction wheel is a "black box" with an output vibration signature. Magnetic-bearings reaction wheels have been proposed to mitigate these problems.[39] Other sources of vibrations in spacecraft are the turbulent flow of coolant or fuel, propulsive burns, composite microcracking, and any other mechanism with moving parts. Another source of jitter is micrometeoroid or orbital debris impact, which causes a transfer of momentum from the impactor to the spacecraft.[40]

In general, any release of energy through vibration would fall into this category, but again sources that are specifically due to microdynamics or thermal disturbances will be treated separately in this paper in Secs. 2.4 and 2.8.

In general, the jitter environment of an instrument will largely determine the stiffness and damping requirements of the structure. Note that both stiffness[41] and damping[42] of a material are temperature-dependent and therefore the dynamics of the structure is subject to a change depending on its operational temperature. Measurement of these properties may also require special instrumentation capable of operating at extreme temperatures.[43] In practice, a stable structure is typically as stiff as required and as lightweight as possible. These conflicting requirements define the trade-off of structural design, as more stiffness requires either more load-carrying material or a more efficient use of it. However, the specific stiffness of materials or structural depth is not easily scalable with the size of the observatory.[16,44] Structural depth also requires either a large volume or complex deployment mechanisms, which add hysteresis and uncertainty to the deployment.

2.6 *Thermal Cycling and Creep*

Thermal effects can produce misalignment of components. This can happen in a reversible way, as is the case of thermal expansion, or irreversibly, in case of creep. Both effects are critical to the operation of space instruments. In addition to misalignment, the refractive index of lenses, beam splitters, and other refractive elements can change as a function of temperature. Refractive elements, however, are not usually part of the OTE of deployable space instruments, which is the focus of this paper.

The main drivers of the thermal environment of a spacecraft are the heat dissipation of its components, its injection and operational orbits, and its ability to reject or absorb radiation. A spacecraft in orbit cannot evacuate the heat it produces or receives by any other means than radiation heat exchange. Ideally, it would be possible to size and align the structure of a space optical system such that the instrument would reach radiative equilibrium with its environment at its nominal alignment. This is not possible because of the dynamic nature of heat inputs to the system and the uncertainty in its modeling.

Thermal expansion is described by the material's coefficient of thermal expansion (CTE). Thermal expansion over wide ranges of temperature, however, does not behave in a linear way. CTEs reported in the literature are usually specified for a certain temperature, such as ambient temperatures. This is not necessarily the operating temperature of the structure. Some telescopes have a certain temperature range required to operate, such as thermal IR telescopes,[45] while others are indifferent to it, but their temperature is defined primarily by their environment. Therefore, it is of primary importance to utilize the correct temperature to linearize the thermal expansion behavior of the material. In general, thermal expansion is an undesirable effect, which makes very low CTEs desirable when choosing materials. In some cases, high CTE materials can be used for passive compensation techniques.[2]

Another effect of thermal expansion is thermal warping or bending, which is the result of the combination of thermal expansion and the uneven distribution of temperatures in a bulk component. Even if a certain component achieves perfect radiative or conductive equilibrium with its environment, there can be a temperature gradient within the material, which makes a region expand or contract more than others. This is typical of situations where a component receives heat from one side and emits it on a colder side. This induces a global bending of the component. This bending may be completely acceptable if it has been modeled and included in the design previously. However, changes to these gradients will negate this compensation. Both the magnitude and variability of these gradients are diminished by high conductivity materials for given boundary conditions. Homogeneous temperature changes also allow an easier definition of the structure's thermal center, which may assist in the modeling stages. Materials with high thermal conductivity, which favor a homogeneous temperature distribution, are therefore desirable.

Taking these two effects into account, a coefficient of thermal warping can be defined as α/κ, with α being the materials' CTE and κ its thermal conductivity. This gives a measure of how different materials would tend to warp[46,47] for a given heat transfer situation. Another figure of merit is described by Bely[2] and defined as $\kappa/\alpha C_p \rho$. This parameter includes a correction for thermal diffusivity, which is the conductivity divided over material's density ρ and its specific heat C_p. This is done in order to describe how quickly the steady state is reached after a change in

the boundary conditions of the thermal property. Note the behavior of this parameter is inverse to the aforementioned coefficient of thermal warping.

A high thermal diffusivity and therefore fast response to thermal variation may not be desirable if the system is designed to be heavily damped through the use of a large thermal mass or latent heat storage. In that case, these compound figures of merit for a material may have their meaning inverted or may be ignored. However, the use of high thermal mass systems typically imply larger inertial mass and volume, partially negating the benefits of deployable systems in space applications. A compromise solution may be found in the use of phase-change materials, which allow additional heat to be used in a reversible phase transition without the need for a large mass.[48]

2.7 *Thermal Flutter*

Thermal flutter can be understood as a dynamic effect caused by cycles of thermal warping, exciting vibration modes of the system. The Hubble Space Telescope famously experienced a disturbance in its pointing whenever undergoing eclipse due to quick heating and deformation of the deployable solar panels, which excited structural modes.[49,50] Deployable optics, as discussed in Sec. 2.3, tend to have lower eigenfrequencies, possibly by 2 orders of magnitude, and tend to be more exposed to thermal fluxes than traditional monolithic telescopes, which are encased in rigid bodies. A way to mitigate this effect is keeping heat fluxes steady by means of a thermal shield or particular orbit selection, or diminishing the aforementioned effects of thermal expansion. For missions that orbit Lagrange points, the solar heat flux remains constant and therefore flutter is not a concern. Thermal flutter can affect the pointing stability of instruments or cause instability of the optical system itself, introducing wavefront jitter.

The overall phenomenon can be explained with a boom exposed to solar fluxes. Limited thermal conductivity will establish a steep temperature difference between the exposed and shaded sides, which causes the former to expand more than the latter. If the process can be regarded as quasistatic, no dynamic effect will occur. However, booms might be poorly insulated and have small thermal inertia, in addition to low eigenfrequencies. Boley[51] proposed that the coupling between thermal fluxes and vibration modes may be assessed through the parameter:

$$B = \frac{t_T}{t_M}, \tag{1}$$

where t_T is the characteristic thermal time and t_M is a characteristic time of the dynamic response, usually the inverse of the first natural frequency of the system. A way to assess this effect is to consider the amplification factor:

$$R = 1 + \frac{1}{\sqrt{1 + B^2}}, \tag{2}$$

which gives a magnitude of the dynamic effect compared to the quasistatic case. This classical approach has been cited as adequate for engineering purposes[52] but is also extended to other situations, such as functionally graded beams[53] or plates.[54]

2.8 *Thermal Creaking*

The other major coupled effect is referred to in the literature as thermal creaking or snapping. This refers to differential heating of contact interfaces causing a vibration as stresses built up at the interface are violently released.

Kim[55] studied the interaction between this phenomenon and the dynamics of spacecraft. This phenomenon happens primarily in the joints of deployable structures due to the presence of contact interfaces. In essence, the energy release mechanisms are the same as described in Sec. 2.4, but the driver of the stress accumulation is the constrained thermal expansion. In terms of mitigation, the same recommendations as exposed in Sec. 2.4 apply.

Since differential thermal expansion is the driver of this phenomenon, limiting the temperature difference across a contact interface with the same materials on both elements can prevent slippage. This, however, is not easily achieved in mechanisms with nonconforming contact, as it is usually the contact itself that acts as a thermal interface. These contact interfaces in precision applications usually rely on point or line contacts,[56] which minimizes the effective thermal contact area. In contact interfaces that have different materials, the CTE mismatch between them will drive slippage proportional to a bulk temperature change of the whole joint, even if the temperatures across the interface are the same.

3 State of the Art in Deployable Space Optics

In this section, proposed systems implementing deployable space optics are summarized. Special attention is given to its thermal and mechanical descriptions. This will bring insight as to the level of maturity of the project and the focus of its researchers. There is a great diversity in both the characteristics and maturity of these projects, some of which are complex design exercises. Others have been developed to completion or have prospects of doing so.

In this section, the observatories have been categorized on three classes, namely the L2 observatories, the LEO telescopes deploying along its optical axis, and the LEO telescopes, which deploy their primary mirror. No observatories have been proposed in higher Earth orbits, moon orbits, or heliocentric orbits. From a mechanical perspective, these other points negate the advantage of LEO for EO purposes, and diminish the advantages of L2 for astronomy, without foreseeable benefit. This also points to an increasing diversification in the topology of space optics missions.

3.1 *Large Lagrange Point 2 Observatories*

The L2 observatories are missions that employ telescopes that do not fit in existing launchers and orbit the second Sun–Earth Lagrange point. Their mission is to look into the universe for a number of scientific enquiries. They have the largest aperture sizes, which need to be deployed in order to fit the launcher, and the largest focal length, which is also deployed. Two such missions are present in the literature: The JWST and the Large Ultraviolet and Infrared Surveyor (LUVOIR). Their thermal environment in L2 is stable save for fluctuations in solar output, which eliminate concerns of thermal flutter and mitigate temperature variations. The large structures of these missions and their use of many mirror segments, however, exacerbate wavefront stability challenges. Their stringent WFE budget, resulting directly from the scientific requirements, imposes the need for more complicated alignment and vibration isolation mechanisms. Owing to their complexity and institutional support, these are the most well-documented and extensively researched projects reported so far in the literature.

In these missions, microdynamics is a major concern due to the large number of interfaces, joints, and latches involved, and much of the knowledge presented in Sec. 2.4 is derived directly from investigations performed to develop JWST.

3.1.1 *James Webb Space Telescope*

The JWST is the largest and most complex deployable optics instrument built so far. Here, a summary of the key thermomechanical elements of its OTE is presented. JWST will operate in orbit around the second Earth–Sun Lagrange point (L2). This provides a stable thermal environment compared to the eclipse cycles, which occur in orbit around Earth. Figure 3 shows an exploded view of the JWST's OTE plus the integrated science module and the thermal management system, and a schematic of the sunshield.

Optical design. JWST is a three-mirror anastigmat (TMA) with a segmented and actuated primary mirror (M1), 6.5 m across, an actuated secondary (M2), and a fast steering mirror incorporated in the exit pupil for line-of-sight disturbance correction. The dimensions of the primary mirror and the sunshield exceed those of the largest launchers in the market. The telescope

observes in visible and IR wavelengths, being diffraction limited at 2 μm. The need for operating wavelengths in the thermal IR range also imposes operational temperatures in the order of 40 to 60 K, to prevent emissions from the telescope from affecting the signal.

Describing JWST or any of its subsystems in full is well beyond the scope of this paper. A wealth of information can be found in the literature. Howard et al.[59–64] describe in more detail the optical design and the linear optical model developed to run structural–thermal–optical performance analysis on it.[34,65] A summary of Howard's papers was published in 2011.[66] Here the most relevant aspects of its design will be outlined: mirrors, deployment mechanisms, fine actuation mechanism, and the sunshield.

Mirror technology. The JWST mirrors are made of beryllium O-30-H.[67] While beryllium has a relatively poor thermal stability at ambient temperatures, its total thermal expansion is very small when cooled to JWST's cryogenic operational temperatures. It is also very lightweight, strong, and has good thermal conductivity, compared to other optical materials. Material was removed from the mirror cores to produce a rib structure that is both lightweight and stiff. When compared with the competing material, ultralow expansion (ULE™) glass, beryllium was selected for its superior technical properties. This decision was made despite the fact that beryllium posed higher risks of production delays and cost overruns.[67]

Deployment mechanism. The segmented mirrors are mounted in a central, static frame, and two "wings," which have to deploy over a 103-deg angle and latch in place, powered by a stepper motor. Both the fixed and mobile frames are made of carbon fiber composites, specifically tuned for thermal stability through manipulation of the material CTE.[68] This is done in order to minimize temperature dependence of the final positions of the mirrors. The development team observed the principles previously laid out to avoid microdynamics response. Nonconforming interfaces were used so as to avoid any load transfer through friction and subsequent microslippage. However, stiffness requirements for some interfaces made it necessary to add redundant nonconforming contacts or oversized friction joints.[69]

Actuation mechanism. Deployment repeatability requirements for this system, from the launch stowed position to the nominally deployed operational position, are in the order of a few millimeters.[69] This is a very large error compared to the allowable WFE in practice. The mirror positioning is corrected by the actuation mechanism down to a step size smaller than 10 nm. This is achieved through the use of a two-stage actuation mechanism, with a coarse range of 20 and a fine range of 2 μm. The actuators are mounted on a beryllium delta frame and interface with the mirror in a hexapod configuration, which provides 6 DOFs position control. An additional actuator, coupled to beryllium struts, also provides radius of curvature correction.[70] The overall control architecture is described by Scott Knight et al.[71] The actuators are powered by a so-called gear motor, composed of a stepper motor, a resolver, and a gear head. The bearings in the motor are a limited lifetime item, sized for the expected mission lifetime.[57]

Sunshield. Passive cooling of the JWST's OTE will be achieved mainly through the use of a large, deployable sunshield, as shown in Fig. 3, which stands between the Sun and the OTIS, which is the OTE plus the Integrated Science module. The sunshield is composed of five layers of Kapton E with a vapor-deposited aluminum (VDA) coating on their inner faces. In the outer faces, the two outer layers are coated with a silicon optical solar reflector coating, and the three inner faces with the same VDA. The layers are arranged with a dihedral angle, which allows radial rejection of heat both from the spacecraft and from sunlight.[58] The sunshield is intended to receive roughly 300 kW of thermal power on its hot side but let less than 0.05 W pass on to the cold side.[72] The sunshield is deployed via four hinged booms and two additional telescopic booms. These six booms are attached to tensioning mechanisms, which are in charge of separating and stretching the different layers of the shield to its designated geometry.

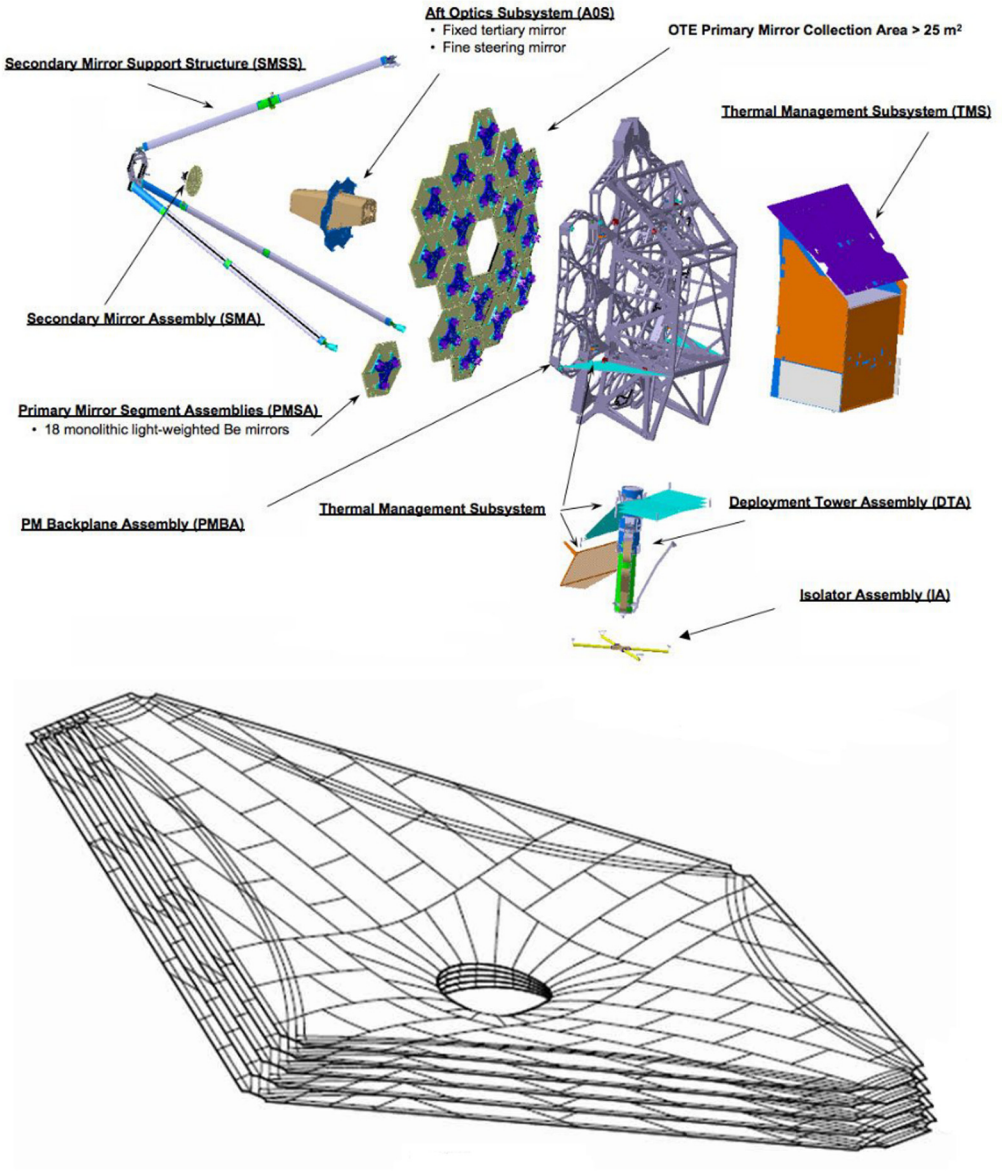

Fig. 3 (Top) Exploded view of the main elements of JWST, including the integrated science module and the thermal management unit.[57] (Bottom) Schematic representation of JWST's sunshield.[58]

3.1.2 *Large Ultraviolet Optical Infrared Surveyor*

LUVOIR is not, strictly speaking, a definite project but rather a response to the call for proposals initiated by NASA as part of its decadal survey on astronomy missions. Similar concepts for very large telescopes operating in the ultraviolet, visible and near infrared have been proposed prior to the current LUVOIR design. Two notable concepts are the Advanced Technology Large-Aperture Space Telescope (ATLAST) and the High Definition Space Telescope (HDST), but these offer less engineering analysis.[73] At the same time, LUVOIR is one of the competing proposals for prioritization of the next large observatories, alongside the Origins Space Telescope (OST), Habitable Exoplanet Imaging Mission (HabEx), and the Lynx X-ray Observatory. Of these concepts, only LUVOIR has seen extensive development in the direction of a segmented aperture deployable architecture like that of the JWST. However, a concept for a smaller version of HabEx called HabEx Lite was proposed[74] featuring a segmented but nondeployable primary mirror. OST also is also meant to use a non-deployable, segmented primary mirror.[75]

LUVOIR has been proposed in different formats, including one featuring a monolithic 8 m primary mirror. However, most of the proposals follow the trend toward a segmented aperture

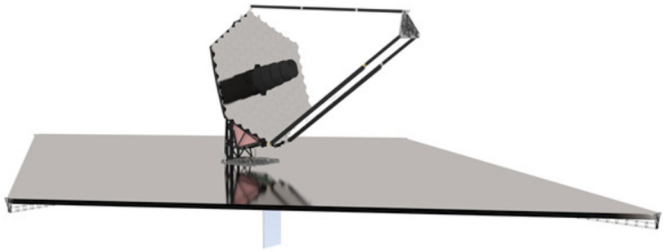

Fig. 4 LUVOIR-A conceptual architecture.[78]

reminiscent of that of JWST but substantially larger. This would allow to employ the lessons learned during development of JWST but also tightens the alignment requirements by a factor of approximately 4 based on a diffraction limit at 500 nm.[16] Proposals exist for primary mirrors of sizes 9.2, 11.7, and 16.8 m.[76] Any of these proposals exceeds the total diameter of any current launcher fairing. The latest report available[77] further develops a 15-m aperture concept as LUVOIR-A, which can be seen in Fig. 4. Another possible architecture described in that report, LUVOIR-B, is based on an 8-m primary aperture, off-axis telescope.

As its name implies, this telescope would operate primarily in the optical range, with capabilities in ultraviolet and shortwave IR, therefore, being a true successor to the Hubble Space Telescope. This means that it would be a "warm" telescope, without the need to create a cryogenic environment. Even so, operation of this telescope will require launching it into an orbit about the L2 Lagrange point, and a large sunshade to prevent sunlight from affecting the measurements. The requirements for this sunshade are likely to be simpler than those of JWST's sunshield.[79]

The architecture for the current LUVOIR-A concept consists of a 120-segment primary mirror aperture, with all segments controlled in 6 DOFs. The use of ULE™ segments in a closed back structure makes these segments stiffer than their JWST predecessors, and so the shape actuator can be dropped.[78] Like in JWST, a fine steering mirror would provide line of sight correction. LUVOIR-B is an off-axis TMA telescope with 55 mirror segments, also controlled in 6 DOFs. The deployment mechanisms of either concept are broadly based on the wings.

In addition to controlling the rigid body motions of the primary mirror segments and the secondary mirror, LUVOIR is also meant to control the temperature of each individual segment via the use of heater and diffuser plates mounted behind each segment.[80]

3.2 *Earth-Orbiting Observatories Deploying along Optical Axis*

These missions are small satellites intended to deploy an element along its main axis with the intention of achieving longer focal lengths than would otherwise be possible in a constrained space. However, not deploying the primary aperture, the achievable aperture and therefore achievable image quality is limited. This can be mitigated by having these instruments fly on very low altitudes, which makes their service life limited.

This is the simplest possibility for deployment, and it has attracted interest from companies and universities because it is potentially the cheapest and fastest technology for development purposes. From a mechanical perspective, these configurations suffer from low eigenfrequencies in the bending of elements along the optical axis. This makes it difficult to keep the alignment of the main optical elements and precisely control their attitude. However, not having a segmented aperture, these systems would not need to cope with wavefront stability issues due to alignment of mirror segments. This architecture also simplifies the design process of a baffle for straylight and thermal control, which can be simply attached to the deployable element. The reduced amount of deployment mechanisms also reduces the induced microdynamic instabilities.

3.2.1 *Dobson Space Telescope*

Another project, which saw development during the 2000s, was the Dobson Space Telescope (DoST), by a team of researcher at TU Berlin. This project was reported on by Segert et al.[81,82] They claimed VHR capabilities from a Microsat platform flying at 550 km, and dual EO and near-Earth object observation purposes. The primary mirror aperture was of 0.5 m for its baseline

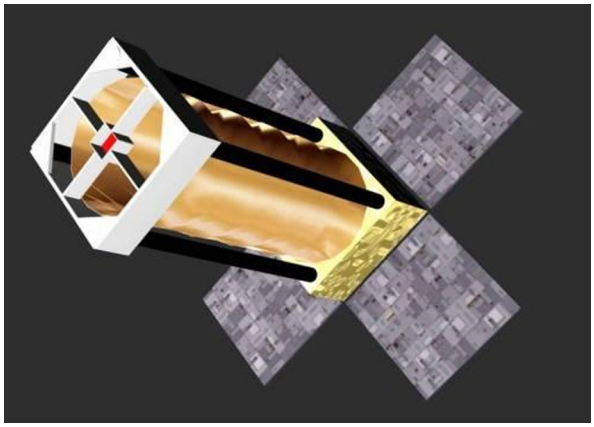

Fig. 5 Artist impression of the deployed DoST.[83]

mission. The operational wavelength is not detailed in the papers, but it is understood to cover the visible range. The project was reported on over a series of papers, including several experimental setups and a tentative launch date in 2012. The members of the team moved on to create the startup Berlin Space Technologies GmbH, which aimed to take the project to the market, but the company does not list deployable telescopes as part of their product line. The project was eventually discontinued because it was not deemed commercially viable.

In the case of the DoST architecture, only the secondary mirror is stowed for launch and deployed in orbit. This allows for a longer focal length with a significant reduction in size, at least in one dimension. The deployment is achieved with a rigid deployable truss, which pushes the secondary mirror 1.1 m away from its stowed position, though this mechanism is not explained in detail. The fact that there is no segmented aperture makes misalignment much less critical. The DoST implements an active optics strategy with a 6 DOFs-actuated secondary mirror. A baffle incorporated in the secondary mirror structure also provides cover for the primary mirror, and the active optics mechanism is expected to bring the errors due to deployment repeatability and thermal expansion from 1 mm to 1 μm. The DoST concept is shown in Fig. 5.

3.2.2 *Collapsible Space Telescope*

Yet another project for deployable optics can be found in the Collapsible Space Telescope (CST) project, a proposal for a deployable secondary mirror mounted on a coiled mast.[84] The operational wavelength of this telescope is not detailed, other than covering the visible range. A baseline primary aperture of 152.2 mm was proposed to fly at an altitude of 250 km. The overall architecture of this system is similar to that of the DoST and is shown in Fig. 6. Once released, the strain energy stored in the coils pushes the secondary mirror away from the primary. This technique does not affect the aperture of the entrance pupil and therefore does not increase the achievable diffraction-limited resolution but makes integration of a baffle easy and dramatically increases the achievable focal length. This project is scarcely reported and does not have any continuation beyond the original paper, which is a valid conceptual design case but lacks sufficient analysis to back up its feasibility.

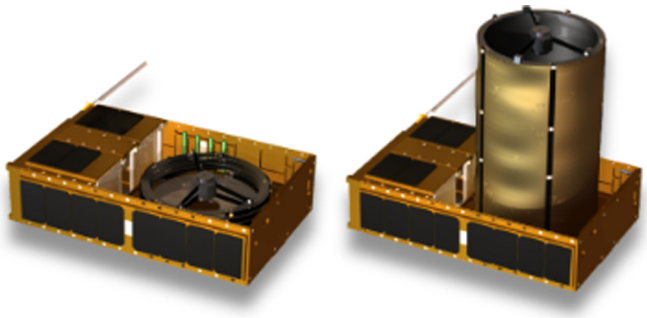

Fig. 6 CST concept, showing the deployment sequence.[84]

Fig. 7 Concept of the SSTL telescopic deployment barrel.[6]

3.2.3 *Surrey Satellite Technologies Limited deployable telescope*

Surrey Satellite Technologies Limited (SSTL) proposed a telescopic optical barrel, shown in Fig. 7 coupled to the secondary mirror of a Cassegrain telescope. The system performs at a GSD of 1 m and is built upon heritage of their Carbonite-2 satellite but with a deployable secondary mirror. This is estimated to lower the volume requirements of each system inside the launcher fairing, thereby allowing for more deployments with less launches. Gooding[6] proposes a case study with a 500 km baseline orbit, though no details of operational wavelength, focal length, or primary aperture are provided.

The secondary mirror is spherical, which restricts the alignment procedure to a 3 DOFs kinematic problem. The same optical barrel used to deploy the secondary mirror provides protection for the primary mirror and is a straylight management tool. The barrel deployment is powered by a motor that drives a lead screw per barrel section into a V groove. The primary mirror is monolithic, and so the maximum aperture is still limited by the available volume within the fairing. The focal length, however, can be drastically increased similarly to that of the CST and the DoST.

3.2.4 *Picosatellite for Remote Sensing and Innovative Space Missions*

The Japanese Picosatellite for Remote Sensing and Innovative Space Missions (PRISM)[85] is, to the best of the author's knowledge, the only deployable optics spacecraft whose launch has

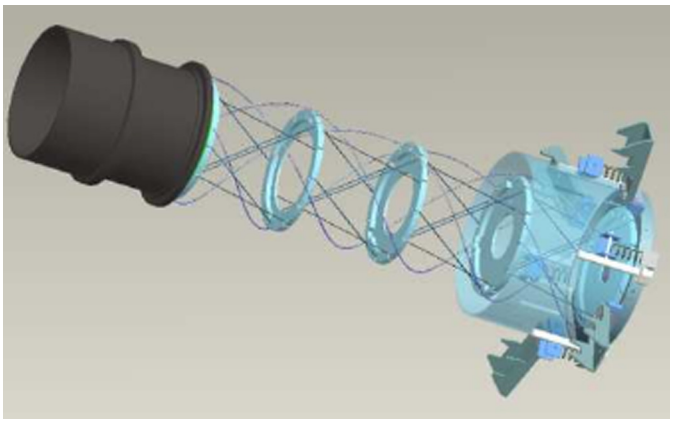

Fig. 8 Schematic representation of PRISM, showing the coil booms that push the focusing lens away. The baffle is omitted for clarity.[85]

been confirmed. It was successfully inserted in a 660-km circular orbit in 2008, as a technology demonstrator for a nanosatellite class imager. Unlike all other examples cited herein, PRISM is a refractive system with an aperture of 90 mm.[85] The overall system is shown in Fig. 8.

The optical system is pushed away from the main instrument housing by means of a collapsible boom, similar to the mechanism described in the case of the CST.[86] This allows the system to achieve a much longer focal length than would otherwise be possible. The coils are also used to pull a baffle, which provides straylight control and a degree of thermal protection to the structure. The detector array is mounted in a focusing mechanism, which can adjust its position to correct for focus errors caused by the flexible deployable structure.[85] The low stiffness structure made special correction of its line of sight jitter necessary,[87] but successful imaging with 30-m GSD was achieved.

3.3 *Earth-Orbiting Observatories with Segmented Apertures*

These systems are proposed to deploy the primary mirror and may or may not deploy the secondary mirror. In this way, they can increase both the focal length and the aperture of the optical system beyond what is achievable with a conventional telescope of the same size. They are also smaller than the L2 observatories, although eclipses are present in their thermal environment. The alignment of primary mirror segments is therefore critical, and disturbances are frequent. The solution is generally the use of active optics mechanisms, which constantly correct the alignment.

The challenges of telescopes that only deploy along their optical axis also apply here, but they are aggravated by the difficulty to integrate a baffle to mitigate the large amounts of straylight from albedo originated outside of the field of view and the thermal influence of the solar flux.

3.3.1 *Large Aperture Telescope Technology*

The Large Aperture Telescope Technology (LATT) project is reported by Marchi et al. (2008) in several papers. Its purpose was described by Hallibert and Marchi[88] as pushing the critical technology readiness level (TRL) of large active mirrors, taking advantage of existing experience with active secondary mirrors for ground-based observatories. The project was finalized in 2015, considering the technology for large-aperture active mirrors to be TRL 5 under the European Space Agency standard.

LATT proposed a design of an afocal telescope with 4 m of aperture diameter to take differential absorption Lidar measurements around the 935-nm wavelength. Unlike the rest of the telescopes mentioned herein, this telescope's purpose is not imaging, and it doesn't operate within the visible spectrum.[89] The design featured a segmented primary mirror with active segments made with a CFRP core and a thin sheet of Zerodur. A novel feature of the design is the use of voice coil actuators to make the large aperture mirror correct its shape. In addition, electrostatic locking is proposed as a means of holding the thin sheet to the substrate, providing a strong load-path to resist launch loads.

The deployment of these mirrors relies on elastic memory composite hinges. The authors proposed that the error inherent to this technology could be compensated by means of the actuators. In addition, the design featured an inflatable baffle, which covered the entire system in order to prevent straylight from falling in the detector.[89] The complete concept can be seen in Fig. 9. An alternative design was proposed by Thompson et al.[91]

Its purpose it to push the critical TRLs for a near-infrared (NIR), very large aperture telescope. Their progress reports a very lightweight active mirror, and an optical design featuring an 7-m^2 deployable collection area. Though some of the technical requirements of this project have been published, there is no publicly available information about its phasing budget. Details on its operational orbit are not explicitly reported, though calculations for straylight reported by Mazzinghi et al.[92] point to a 450-km altitude.

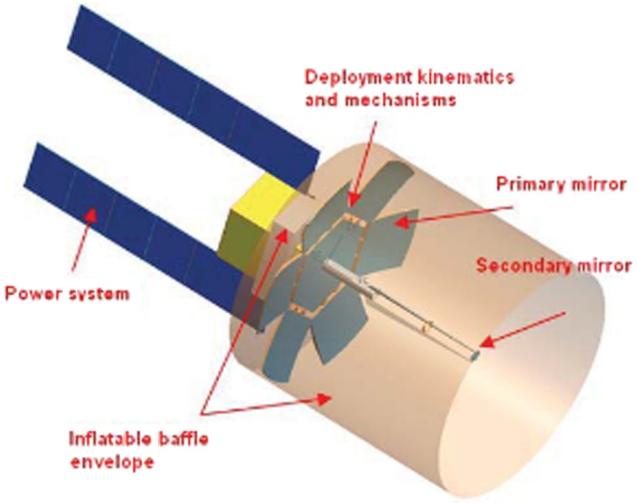

Fig. 9 System architecture of the LATT baseline telescope, showing the cylindrical baffle.[90]

3.3.2 *Deployable Petal Telescope*

Utah State University's Space Dynamics Lab built and tested the so-called Deployable Petal Telescope (DPT),[93] a Cassegrain telescope, which can be mounted on a 3-U CubeSat platform, deploying both its primary and secondary mirrors. This endeavor, however, is scarcely reported on the literature, and so actual feasibility and performance of the system is difficult to ascertain. A video is still available online, in which the primary mirror segments are seen to unfold in a flower-like fashion, whereas the secondary mirror, mounted on a rail, deploys away from the instrument housing.

The DPT is a Cassegrain-type telescope with a 200-mm aperture, deployable segmented primary mirror, which unfolds in a similar fashion to flower petals. The prototype mirror is a smaller version and has flat at the tip to aid in alignment, which makes its effective aperture smaller. The secondary mirror is mounted on a rail, which linearly extends away from the primary. Both mechanisms are described to be fully passive via a spring load. The conceptual imaging system is diffraction limited at 632.8 nm, achieving a 1.3-GSD from a 500-km orbital altitude. In the architecture reported by Champagne et al.,[93] there are no external baffles, but a collapsible baffle is installed in the space between the two mirrors. This would mean the telescope is largely exposed to heat fluxes from the Sun. Unlike most of the other deployable telescopes, the DPT does not implement an active optics mechanism to correct for misalignment or

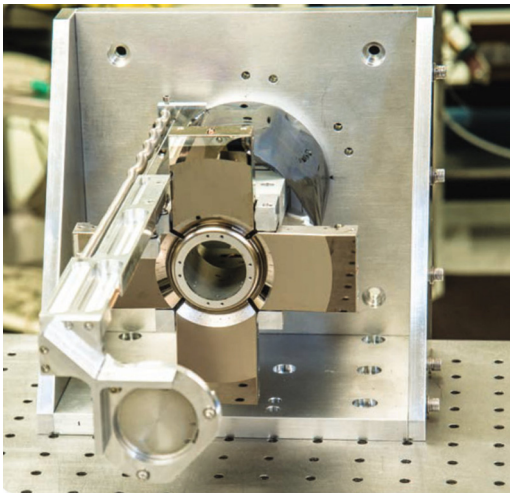

Fig. 10 Picture of the DPT test setup, not including the internal baffles.[94]

nonrepeatability. The authors trust the assembly to be stable enough in 5 DOFs, excluding the tip motion, which is adjusted through a mechanism attached to the back of the mirror. This mechanism was tested for deployment repeatability and the results showed that most of the surface error came from the individual segments, which the authors expected could be improved. The test setup for the DPT is shown in Fig. 10.

3.3.3 *Deployable Space Telescope (UK Astronomy Technology Centre)*

A more recent attempt to use CubeSats for VHR EO is reported by Schwartz et al.[95] The purpose of this project is to reach a 39-cm GSD from a CubeSat platform flying at 350 km altitude. This system is diffraction limited at 550 nm and has a 300-mm aperture. The authors provide quantified measures of the sensitivity to misalignment of the system and propose an active optics actuation system to get the mirrors aligned within the tolerances. The necessary metrology proposed is a sharpness optimization algorithm, which drives the active optics. The system can fit in a 1.5U CubeSat standard unit. The authors do not describe yet the sensitivity of their concept to thermoelastic deformation as a result of the orbital transients.

The primary mirror active optics acts in tip-tilt and piston directions. Three motors are coupled to the mirror by means of a flexure system connected to a steel shaft. This shaft acts as the connection to the mirror substrate and also integrates a torsion spring that powers the deployment. The active optics strategy is able to obtain a surface error of 25 nm under laboratory conditions.[96] The authors do not report on a particular deployment strategy for the secondary mirror. In the latest design, as shown in Fig. 11, a baffle is included in between the primary and secondary mirrors for straylight attenuation, which seems to leave the telescope exposed to thermal fluxes like in the DPT case.

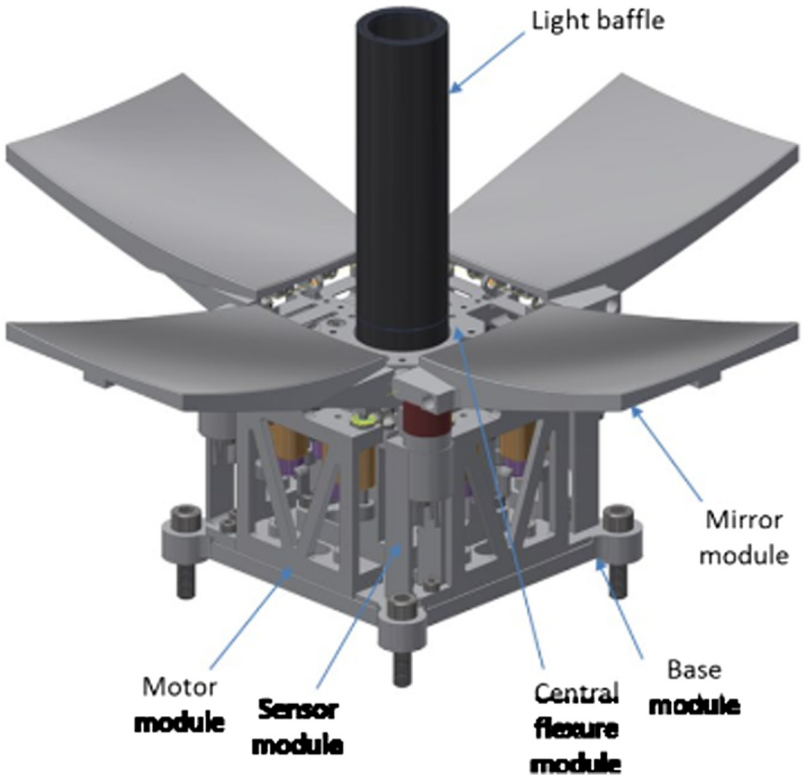

Fig. 11 Schematic representation of the adjustment mechanism of the deployable telescope proposed by Schwartz et al.[95] showing an additional internal baffle.

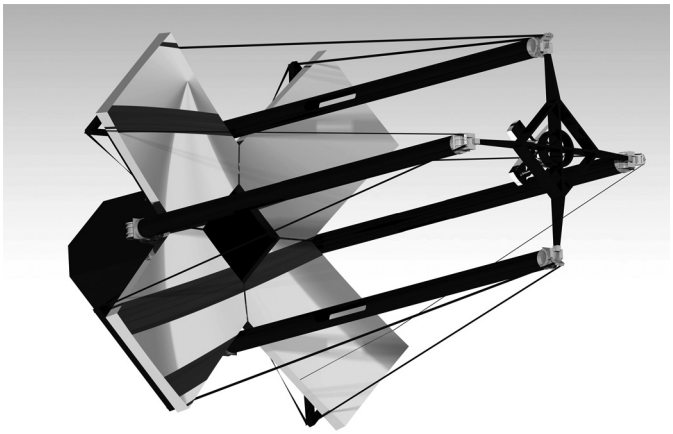

Fig. 12 Artistic rendition of the TUD DST.

3.3.4 *Deployable Space Telescope (TU Delft)*

The TUD DST project was proposed by Kuiper in 2012 and has been running ever since. Dolkens proposed the optical design and a ray-tracing tool to assess its performance. From that, the top–down misalignment budgets were derived and presented in Ref. 97. In addition to the optical analysis, several Master of Science theses have been published by the TU Delft,[98–102] detailing the evolution of the mechanical design from the first iteration by Dolkens to the latest developments reported by Dolkens et al.[103]

The DST, as shown in Fig. 12, is a TMA telescope with a four-segment primary mirror of 1.5 m aperture, diffraction limited at 550 nm, and flying at 500 km altitude. These segments are actuated in piston and tip-tilt directions, which are regularly identified as the most critical DOFs in both this and other proposals. Aberrations caused by warping of the mirror shape are corrected by a deformable mirror installed in the exit pupil of the OTE. This deformable mirror, however, cannot correct for the WFE caused by a dephasing of the primary mirror. This misalignment is controlled by means of a so-called PistonCam, installed in the intermediate image plane, tracking the sharpness of the image at the mirror edges. This information is fed to a control algorithm, which drives the active optics mechanism.

The mechanical design includes a baffle capable of limiting the variability in the thermal environment and a low hysteresis compliant rolling element hinges, so as to comply with the guidelines presented in Sec. 2.[99,102] This active optics mechanism was proposed by Pepper.[101] In addition to providing exact constraint and actuation of the mirror substrate to its support plate, the active optics actuator acts as a primary load path holding the mirror through launch with acceptable strength margins. The mechanism consists of four actuators in push–pull configuration, which move an intermediate plate. This intermediate plate is in turn constrained by means of a hexapod mount to the mirror substrate.

Successful operation of the system relies on three layers of increasingly strict tolerances.[97] The deployment mechanism should be accurate enough to reach a coarse alignment in the micron range. The system is then actuated to a nominal position in the order of $\lambda/20$, with short WFE jitter disturbances kept below the order of $\lambda/100$, with λ being the diffraction-limited wavelength of the telescope. A deployable structure capable of meeting these requirements taking into consideration all the effects mentioned in this paper and that of Edeson et al.[8] is currently under development.

3.3.5 *Deployable Optics Model Experiment*

The Deployable Optics Model Experiment (DOME), reported by Peterson and Hinkle, was a structural mechanics experiment related to a concept differential absorption Lidar deployable telescope based on the requirements for the Ozone Research through Advanced Cooperative

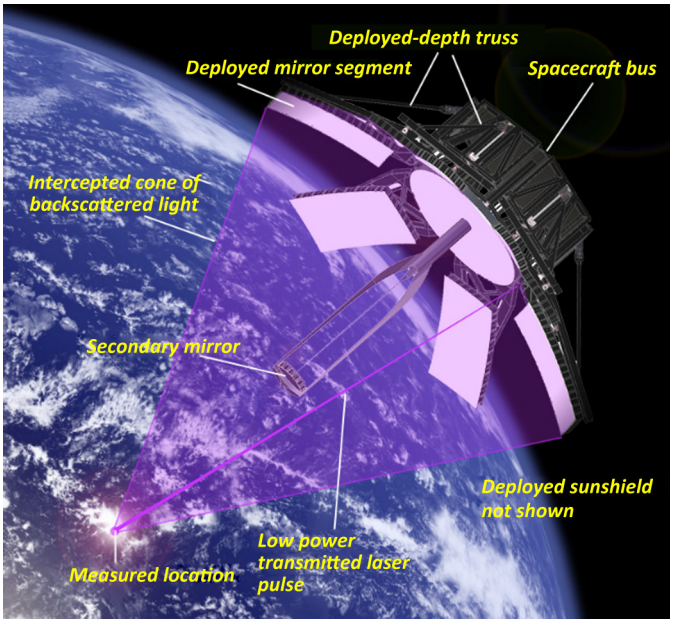

Fig. 13 Artist impression of the Lidar telescope, which was used as baseline by the DOME project.[106]

Lidar Experiments mission.[104,105] The baseline design was a segmented aperture telescope with a 2.55-m diameter consisting of an hexagonal monolithic core and six additional petals. An artist impression of the concept is shown in Fig. 13. Since this was a technology development project, no specific details of orbit or operational wavelength are available to the knowledge of the authors.

The purpose of the project was to characterize the behavior of a single deployable petal with a simple deployment mechanism. The mechanism consisted on a strutted hinge, which latched upon reaching the deployed state. Repeatability of the latch was identified as the largest source of deployment nonrepeatability in the mechanism. This meant that the largest effort went to develop a latch with very stringent repeatability requirements.[44] The project was expected to end with the single petal test carried out on this structure coupled to an ultrastable metrology frame. Some results were reported in Ref. 106, but no definite conclusion could be found for the project.

The baseline mirror material for this system is a mixture of CFRP and ULE™.[11,105] The former provides a thermally stable and stiff base, but it does not provide a surface of enough quality. A thin layer of ULE™ is used for that purpose and bonded to the composite mirror core. The mirror core is protected from the effects of moisture through the use of a moisture barrier.[11]

3.3.6 *Deployable In-Space Coherent Imaging Telescope*

The Deployable In-Space Coherent Imaging Telescope (DISCIT) is a project supported by MIT Lincoln Laboratories and the U.S. Air Force. In contrast to the efforts in deployable optics, which were discussed previously, reports related to this project are much sparser in the information about their optical design, focusing more on the development of high-precision deployment mechanisms. However, a ray-trace schematic of the system can be seen in Fig. 14. The researchers intend to reduce the complexity of deployment mechanisms, which can meet optical precision requirements, compared to the complicated deployment mechanism of the JWST.[107]

The baseline optical design is not thoroughly described in the literature available on this project. The objective is a 0.7-m effective sparse aperture Cassegrain telescope.[107] The expected performance of such a system or its operational environment are not clarified either. Some renders related to this project can be found online showing a multimirror arrangement with nondeployable secondary mirror and a deployable, segmented primary. The results of the experiments on the tape spring hinge reported in Ref. 108 show that tape spring hinges can achieve

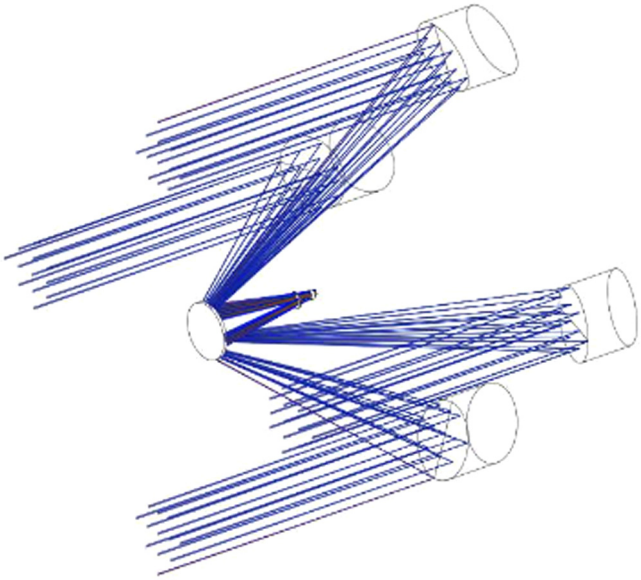

Fig. 14 Optical ray tracing schematic of DISCIT's baseline optical architecture.[107]

micron-level repeatability and also provide interesting results about their dimensional stability under changes in temperature and humidity.

DISCIT itself does not incorporate any type of baffle as of the current date. A previous project within MIT Lincoln Laboratories, with the involvement of silver, does investigate the deployment of optical barrel assemblies using similar tape spring hinge technology.[109,110] Though this is a separate development to DISCIT, it does mean the authors are aware of the need to baffle sunlight falling onto the telescope.

3.3.7 *Autonomous Assembly Reconfigurable Space Telescope*

Another notable research project is the Autonomous Assembly of a Reconfigurable Space Telescope (AAReST). It has been a long-term student project with students from Caltech supported by the Jet Propulsion Laboratory, and it is expected to be launched in 2020. More than a functional telescope, AAReST is a technology demonstrator for large aperture deformable mirrors and, more importantly, in-orbit reconfiguration of optical segments. The proposed mission has a 0.4-m aperture and operates at the wavelength range of 465 to 615 nm. The main feature of this mission is the detachment of 3U CubeSats called "MirrorSats," which will fly away from the main spacecraft, "CoreSat," achieve reattachment to it at a different location and operate at a 650-km altitude.[111] This sequence is shown in Fig. 15.

Fig. 15 View of the reconfiguration mechanism of AAReST, also showing the integrated tape spring hinge.[112]

The CoreSat mounts two fixed mirrors, whereas the MirrorSats hold a thin-shell CFRP deformable mirror as described by Steeves et al.[113] The large deformable mirrors are mounted on a 3 DOFs platform (piston, tip-tilt) for coarser rigid body motions, providing very high authority control. Reattachment of the MirrorSats is achieved through an electromagnetic docking mechanism, which makes the MirrorSats fall into a Kelvin clamp, which provides a repeatable reattachment.[112] Another valuable element to this mission is the foldable boom, which holds the imaging camera. Mallikarachchi and Pellegrino[114] described the manufacture of the hinges present on these booms. Cutouts on monolithic CFRP booms are made and then bent until the fold. Once the holding force is removed, the strain energy contained in the fold is released, making the boom go back to its original shape with acceptable repeatability.

3.3.8 *UltraLITE*

Ultralightweight Telescope (UltraLITE),[115] also called deployable optical telescope (DOT),[116] is a deployable TMA telescope developed mainly by the Air Force Research Laboratories. This proposed design spawned a series of structure experiments to validate several elements of its architecture. The design featured a deployable tower holding the secondary mirror and three deployable circular mirrors. These mirrors were notable for their very lightweight design, owed to the use of a CFRP core and a thin ULE™ shell, which also acts as an active mirror.[46] This development program focused extensively on active vibration controllers[117] and the design of a very stiff deployment structure through the use of hybrid CFRP, including high and intermediate modulus fibers.[115] Several effective apertures of the telescope were reported throughout the technology development program, with a testbed of 1.7 m being built.[117] More system design options are discussed by Powers et al.[118] for a baseline size of 5 to 6 m apertures flying on high altitudes, in the order of 15,000 km. The precise details of the final design could not be found as to its operating altitude or wavelength, though the latter is understood to be in the visible range.

Catanzaro et al.[46] mentions active heating as thermal control to keep the desirable stability of the telescope. There is no indication that a sunshield or baffle was proposed in the latest embodiment, although early concept schematics showed a deployable one.[118] This is not elaborated in the texts found during this survey. An artist impression of the concept is shown in Fig. 16.

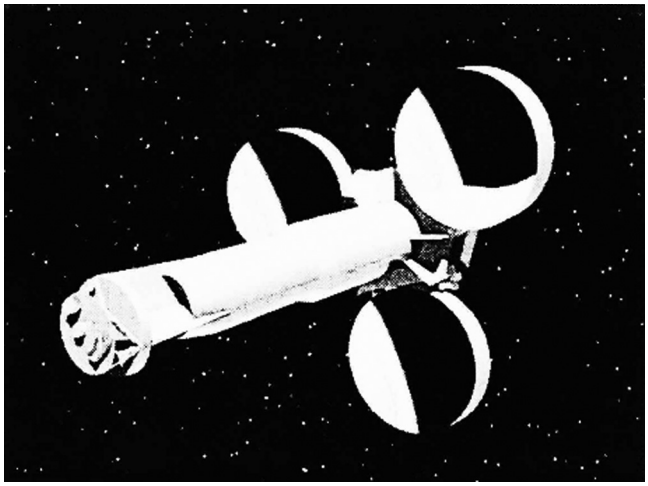

Fig. 16 Artist impression of the UltraLITE telescope.[46]

4 Examination of Critical Technologies

The structural architecture of deployable space optics is determined by the optical characteristics, such as focal length or operating wavelength, and the chosen environment. The observation wavelength is the major defining factor for the alignment requirements, the aperture size, and the instrument's temperature. In addition, the focal length of the system will determine the distance between the major optical elements along the optical axis. These characteristics give rise to a diversity of possible designs, but this section intends to summarize the technologies that underlie them. Table 1 summarizes the aforementioned projects along with their main characteristics. As this table shows, most of the telescopes proposed are based either on a Cassegrain or TMA configurations, which are fully reflective and therefore avoid chromatic aberrations. The exceptions to this are AAReST and PRISM, which incorporate refractive elements.

While there are many projects, not all of the institutions sponsoring them have the resources to bring them to completion. From the review performed, only JWST and LUVOIR have been extensively documented in all the aspects of design from the optics to the structural mechanics and actuation. PRISM is notable for being the first deployable optical experiment, but its documentation explains more about the control of the focusing mechanism and attitude than the thermomechanical requirements.[85] Other projects have achieved partial hardware demonstrations, showing particular aspects of their technology but not a systematic approach to addressing the issues highlighted herein. Some of this is possibly attributable to a willingness to withhold information from the public domain.

4.1 *Deployment Mechanisms and the Need for Active Optics*

There are 2 orders of magnitude differences between achievable deployment repeatability and the allowable WFE for high-quality imaging in visual and NIR ranges. Deployment repeatability depends on the specific technology, which locks the structure in place, and on the size of the structure, with typical values in the order of a few micrometers.[33,119] For comparison, WFE requirements for diffraction-limited optics are in the order of 10s of nanometers.[120] In addition, in-orbit disturbances can affect the stability of the system in several timescales. Therefore, there is a need for active correction of at least the most sensitive DOF, which can be determined via optical sensitivity analysis. In the most demanding applications, full 6 DOFs per element control and shape control are required. The total stroke of such a system must be matched to the magnitude of the foreseeable disturbances, and its resolution must be smaller than the allowable WFE.

This is indeed the overall consensus in the deployable optics literature, with projects that either focus heavily on the development of novel active optics concepts or acknowledge it as an essential enabler to achieve its goals. This holds true, regardless of the overall size of the proposed telescope and its environment. Table 1 shows how the majority of systems include some type of active correction, although some do not specify whether or not they do. Lake et al.[121] highlighted the importance of a trade-off between structural stiffness requirements and authority of the control system. Most active optics mechanisms allow for more DOFs than the six per element pure rigid body kinematics by exerting some control over the surface shape. This can be achieved at the primary optical element or through the use of a deformable mirror as is the case of the TU Delft DST. JWST implements one extra DOF per mirror segment for radius of curvature control of the primary mirror. AAReST and LATT propose a fully deformable primary mirror with an undefined number of DOFs, which allows much more control authority.

Survivability of these large active mirrors can be achieved through electrostatic locking of the face sheet during launch.[90] With this technology, extremely low areal densities, below 20 kg/m^2 can be achieved, however, at the cost of complexity of the active optics mechanisms. However, embodiments such as those in the LATT or AAReST projects are not yet capable of achieving diffraction-limited performance in visible wavelengths.

4.2 *Thermal and Vibration Control*

Thermomechanical stability is achieved through the systematic removal of external influences on the telescope at multiple stages of the mission design. Selecting the environment of the telescope

Table 1 Summary of deployable optics proposed concepts.

Program	Purpose	Wavelength	Environment	Primary aperture	Active optics DOFs	Thermal control technique	Telescope type	Mirror material	Deployables
JWST	ASTRO	IR	L2	6.5 m	132 DOFs[a]	Sunshield	TMA	Beryllium	M1, M2, Sunshield
LUVOIR	ASTRO	VIS	L2	15 to 8 m	726 to 336 DOFs[b]	Sunshade + heating	TMA	ULE™	M1, M2, Sunshield
DoST	ASTRO	VIS	LEO	0.5 m	3 DOFs	Unknown	Cassegrain	Unknown	M2
CST	EO	VIS	LEO	0.15	None	Unknown	Cassegrain	Unknown	M2
SSTL	EO	VIS	LEO	Unknown	3 DOFs	Telescopic baffle	Unknown	Unknown	M2
PRISM	EO	VIS	LEO	0.09 m	1 DOF	Telescopic baffle	Refractive	Glass	Primary lens
LATT	EO	NIR	LEO	4 m	Adaptive mirror	Baffle	Afocal Cassegrain	Zerodur + CFRP	M1
DPT	EO	VIS	LEO	0.2 m	None	Unknown	Cassegrain	Unknown	M1, M2
UK Astro DST	EO	VIS	LEO	0.3 m	12 DOFs	Unknown	Cassegrain	Aluminum	M1
TUD DST	EO	VIS	LEO	1.5 m	12 DOFs	Baffle	TMA	SiC	M1, M2, baffle
DOME	EO	NIR	LEO	2.55[a]	Unknown	Baffle	Unknown	ULE™ + CFRP	M1
DISCIT	EO	VIS	LEO	0.8	Unknown	Unknown	Cassegrain	Unknown	M1
AAReST	ASTRO	VIS	LEO	0.3 m	Adaptive mirror	Active heating	“Prime focus”	Glass-piezoelectric	M1, detector
UltraLITE	EO	VIS	LEO	1.7 m	9 DOFs	Active heating	TMA	ULE™+CFRP	M1

[a]DOFs not including fine steering mirrors.
[b]Controlled DOFs are only for rigid body motions, as LUVOIR does not use radius of curvature control. Prime focus is corrected with additional lenses.

is a choice with many potential variables and trades. Deployable optics in the literature is proposed for either LEO or L2 orbits, parallel to the split between EO purposes and astronomy. Missions in LEO would be primarily for EO, with a focus on lightweight systems that can be produced cheaply, fast, and potentially in larger numbers to provide higher temporal and spatial resolution. L2 is too far away to be a good candidate for EO, but a prime location for astronomy due to a stable thermal environment and constant Sun illumination. Astronomy requires much larger apertures with more stringent optical quality requirements, which results in more complex and sensitive systems in a comparatively milder environment. This divide is clear in Table 1, with the largest apertures and number of controlled DOFs predictably belonging to the large L2 observatories.

In L2, a single sunshield is able to greatly reduce the straylight and thermal effects caused by sunlight, although such sunshield has been a critical part of JWST's development and represents a system of considerable complexity and scale on its own. LEO is a very dynamic environment by comparison due to the need to cope with cycles of dayside and eclipse. A notable exception to this would be the particular case of dawn–dusk Sun-synchronous orbits whose illumination is constant. It is also more populated by orbital debris from previous missions. A large aperture in LEO comes with the need to deploy a baffle to protect it from sunlight if alignment is to be maintained.

In the literature regarding deployable telescopes, thermal stability is addressed mainly through the material choice rather than temperature control of the support structures. LUVOIR is a notable exception to this rule, where active heating is used. Active heating is the simplest way to control the temperature of the optical elements, but it has important drawbacks. Namely it adds to the power requirements of the telescope, is incompatible with cryogenic telescopes, and it increases modeling complexity due to the potential of heat radiating onto other optical assemblies. Eisenhower et al.[80] estimated that for the ATLAST concept, 526.8 W of power would be needed to maintain the correct temperature.

Though this may be attributed to the immaturity of most of the proposals in the literature, there has not been extensive description of a thermal management system and its impacts, with the exception of JWST and LUVOIR.[77] The Delft DST team also considers this a major concern for development.[122,123] This has caused Table 1 to be very incomplete on that aspect.

As for vibration control, there is a need to eliminate or insulate the sources. One area in which this may be achieved is the design of mechanisms that do not transmit any loads through friction[26] and the substitution of classical bearing hinges and joints with compliant mechanisms, which eliminate undesired effects cited in Sec. 2.4, such as creaking, backlash, freeplay, and wear.[124] Owing to the need of pointing the telescope toward the target, reaction wheels will likely be always a necessity, and therefore the microvibration requirements outlined in Sec. 2 must be observed. Deployable optics would benefit from magnetic-bearing or otherwise low-noise reaction wheels, although these are more complex and expensive.

4.3 *Lightweight Mirrors*

Deployable telescopes, compared to monolithic telescopes, have more flexible structures and therefore have comparatively lower eigenfrequencies, which can be partially offset by the use of extremely lightweight, stiff mirrors. Mirror areal density is influenced by total aperture of the segment, available core depth, material choice, and core geometry. Lightweight mirrors can be achieved by removing material from a mirror blank, which achieves bending stiffness by leaving a complex pattern of stiffeners behind the face sheet. This process is limited by manufacturability and local buckling failure modes, if the stiffeners are made excessively thin. Baiocchi and Stahl[16] cite other concerns that may dominate over areal density when deciding on a mirror design, such as stiffness, complexity, and cost.

As for the thermal environment, telescopes operating at cryogenic temperatures benefit from the small cumulative shrinkage of beryllium at cryogenic temperatures, its low density, and high strength.[47] In the case of warm telescopes, beryllium has a relatively high CTE and is typically outperformed by other high performance materials, such as Zerodur, ULE™, and Silicon Carbide (SiC). Zerodur and ULE™ have a long usage history in both ground and space telescopes due to their extremely low CTE at ambient temperature, but they present poor thermal

Table 2 Properties of typical mirror materials.[2,47]

Mirror materials	ρ (kg/m^3)	E (GPa)	σ_{Max} (MPa)	κ (W/m/K)	α (ppm/K)	E/ρ (10^6 m^2/s^2)	σ_{Max}/ρ (10^3 m^2/s^2)	α/κ (m/W)
Borosilicate	2230	63	78	1.2	3.3	28	34,98	2.75
Fused silica	2200	73	48	1.3	0.52	33	34.98	0.4
ULE™	2210	68	50	1.3	0.03	30	22.62	0.023
Zerodur	2530	91	57	1.5	0.05	36	22.53	0.033
CVD SiC	3210	466	440	190	2.2	145	137.07	0.012
Reaction-bonded SiC	2910	360	325.5	155	2.6	124	111.86	0.017
O-30 Beryllium	1850	300	240	216	11.3	162	129.73	0.052
Aluminum	2700	70	310	210	24	26	114.81	0.114
CFRP[a]	1600	160	2100	2	−0.3	100	1312.50	NA

[a]CFRP data are very strongly dependent on the type of fiber and resin, as well as the direction, and it cannot be polished to mirror quality. The numbers for this material are only for comparison purposes to the state of the art, in a direction of interest.

conductivity and are brittle compared to metals or SiC. Another candidate family of materials is aluminum alloys. Aluminum has excellent programmatic and mechanical properties, but it also boasts a much higher CTE than its competitors.[125] However, its good thermal conductivity and the possibility of making its supporting structure out of the same material makes it possible for a full aluminum telescope to have a degree of inherent athermalization, provided the temperature is homogeneous across the entire system. There is little evidence in the literature suggesting that this is enough to offset its high CTE in large aperture telescopes.

Table 2 summarizes the thermal and mechanical properties of these materials. The ρ is the material density, E is the Young's modulus, and σ_{Max} is the maximum allowable stress.

CFRP is used as a base material that can be mixed with an ultralow CTE material, which can be polished in order to profit from the high specific stiffness and thermal stability while preserving the optical surface quality.

The alternative to these stiff mirrors are large active mirrors with very small structural depths, which are controllable through electromechanical actuation to correct for its large initial surface errors, as shown by the LATT and AAReST projects. These are prime examples of the trade-off between mass and control complexity shifting to the latter. So far this approach of very high authority mirror control has not been demonstrated in flight, but experiments have been performed.

5 Summary

In this paper, the main thermomechanical challenges for deployable space optics are described, along with the implementations proposed in 14 different deployable optics missions. While there are large potential gains in mass and volume, system complexity increases substantially. EO systems compensate this drawback through the possibility of multiple deployment or standardized production, whereas astronomical telescopes are enabled to pursue primary apertures beyond the launcher shroud diameter. The fundamental thermomechanical challenges remain the same, although different projects have studied different aspects with special emphasis. The main challenges in thermomechanical design of deployable space optics, from this point of view, are the repeatability of the deployment mechanism, thermal stability, and the use of active optics to compensate for the lack of stiff structures. It is found that thermal stability in particular has been the least extensively described aspect in these projects. The presented results can serve as a starting point on these design considerations. However, system

requirements have a large impact on the key drivers of the design process. The findings presented in this study are being used to direct the development of the Delft University of Technology's DST. In this respect, the development is being steered toward four main technologies: a deployable baffle, which is axisymmetric and acts as thermal shield; compliant element hinges, which are expected to deliver greater deployment repeatability; a fine actuation mechanism for primary mirror segments; and thermal control techniques for passive secondary mirror spiders.

Acknowledgments

The authors would like to thank the support received by Airbus Defence and Space Netherlands via the Dutch TKI funding scheme.

References

1. P. Y. Bely, "The NGST 'Yardstick Mission'," in *The Next Gener. Space Telesc.: Sci. Drivers and Technol. Challenges, 34th Liège Astrophys. Colloq.* (1998).
2. P. Y. Bely, *The Design and Construction of Large Optical Telescopes*, Springer-Verlag, New York (2003).
3. T. H. Zurbuchen, "Summary of NASA responses to Webb independent review board recommendation," Technical Report, NASA (2018).
4. Euroconsult, "Satellite-based Earth observation: market prospects to 2026 (brochure)," Technical Report (2017).
5. DigitalGlobe, "WorldView-4 datasheet," https://www.satimagingcorp.com/satellite-sensors/geoeye-2/ (2016).
6. D. Gooding et al., "A novel deployable telescope to facilitate a low-cost < 1 m GSD video rapid-revisit small satellite constellation," *Proc. SPIE* **11180**, 1118009 (2018).
7. D. Dolkens and J. M. Kuiper, "A deployable telescope for sub-meter resolution from microsatellite platforms," *Proc. SPIE* **10563**, 105633G (2015).
8. R. Edeson, G. S. Aglietti, and A. R.L. Tatnall, "Conventional stable structures for space optics: the state of the art," *Acta Astronaut.* **66**(1–2), 13–32 (2010).
9. W. N. Lai Findley and K. J. S. Onaran, *Creep and Relaxation of Nonlinear Viscoelastic Materials—with an Introduction to Linear Viscoelasticity*, North-Holland Publishing Company, Amsterdam-New York-Oxford (1978).
10. J. C. Machado et al., "Picometer resolution interferometric characterization of the dimensional stability of zero CTE CFRP," *Proc. SPIE* **7018**, 70183D (2008).
11. G. C. Krumweide, "Issues to be addressed in the design and fabrication of ultralightweight meter-class optics," *Proc. SPIE* **3356** (1998).
12. T. J. Bihl, K. D. Pham, and T. W. Murphey, "Modeling and control of active gravity offloading for deployable space structures," *Proc. SPIE* **6555**, 655515 (2007).
13. G. Greschik and W. Keith Belvin, "High-fidelity gravity offloading system for free-free vibration testing," *J. Spacecr. Rockets* **44**(1), 132–142 (2007).
14. M. Schenk and S. D. Guest, "On zero stiffness," *J. Mech. Eng. Sci.* **228**(10), 1701–1714 (2014).
15. O. Han et al., "Gravity-offloading system for large-displacement ground testing of spacecraft mechanisms," in *Proc. 40th Aerosp. Mech. Symp.*, pp. 119–132 (2010).
16. D. Baiocchi and H. P. Stahl, "Enabling future space telescopes: mirror technology review and development roadmap," Astro2010: The Astronomy and Astrophysics Decadal Survey, Technology Development Papers, **23** (2009).
17. E. E. Bloemhof et al., "Extracting the zero-gravity surface figure of a mirror through multiple clockings in a flightlike hexapod mount," *Appl. Opt.* **48**(21), 4239–4245 (2009).
18. F. E. Ostrem, "Transportation and handling loads," Technical Report NASA-SP-8077 (1971).
19. J. Wijker, *Spacecraft Structures*, Springer-Verlag, Berlin Heidelberg (2008).
20. Arianespace, "Ariane 5 user's manual," https://www.arianespace.com/vehicle/ariane-5/ (2004).

21. Arianespace, "Vega user's manual issue 4—revision 0," https://www.arianespace.com/vehicle/vega/# (2014).
22. United Launch Alliance, "Atlas V Launch services user's guide," https://www.ulalaunch.com/rockets/atlas-v (2010).
23. R. Maaß and P. M. Derlet, "Micro-plasticity and recent insights from intermittent and small-scale plasticity," *Acta Mater.* **143**, 338–363 (2017).
24. L. Peterson and J. Hinkle, "Microdynamic design requirements for large space structures," in *44th AIAA/ASME/ASCE/AHS/ASC Struct., Struct. Dyn., and Mater. Conf.*, pp. 1–11 (2003).
25. C. V. White and M. B. Levine, "Microdynamic issues in large deployable space telescopes," *Proc. SPIE* **4198**, 163–171 (2001).
26. M. S. Lake and M. R. Hachkowski, "Design of mechanisms for deployable, optical instruments: guidelines for reducing hysteresis," Technical Report NASA/TM-2000-210089, L-17970, NAS 1.15:210089 (2000).
27. M. D. Ingham and E. F. Crawley, "Microdynamic characterization of modal parameters for a deployable space structure introduction," *AIAA J.* **39**(2), 331–338 (2001).
28. O. Stohlman and S. Pellegrino, "Shape accuracy of a joint-dominated deployable mast," in *51st AIAA/ASME/ASCE/AHS/ASC Struct., Struct. Dyn., and Mater. Conf./18th AIAA/ASME/AHS Adapt. Struct. Conf. 12th*, pp. 1–15 2010.
29. L. M. R. Hardaway and L. D. Peterson, "Nanometer-scale spontaneous vibrations in a deployable truss under mechanical loading," *AIAA J.* **40**(10), 2070–2076 (2002).
30. M. B. Levine, "The interferometry program flight experiments: IPEX I & II," *Proc. SPIE* **3350**, 1–12 (1998).
31. M. S. Lake, P. A. Warren, and L. D. Peterson, "A revolute joint with linear load-displacement response for precision deployable structures," In *37th AIAA/ASME/ASCE.AHS.ASC Struct., Struct. Dyn. and Mater. Conf.*, Salt Lake City (1996).
32. R. N. Coppolino, D. S. Adams, and M. B. Levine, "Midfrequency band dynamics of large space structures," *Proc. SPIE* **5528** (2004).
33. P. A. Warren, L. D. Person, and F. Miller, "Submicron mechanical stability of a prototype deployable space telescope support structure introduction," *J. Spacecr. Rockets* **36**(5), 765–771 (1999).
34. T. T. Hyde et al., "Integrated modeling activities for the James Webb Space Telescope: optical jitter analysis," *Proc. SPIE* **5487**, 1–12 (2004).
35. D. Addari, G. S. Aglietti, and M. Remedia, "Experimental and numerical investigation of coupled microvibration dynamics for satellite reaction wheels," *J. Sound Vib.* **386**, 225–241 (2017).
36. D. K. Kim, "Micro-vibration model and parameter estimation method of a reaction wheel assembly," *J. Sound Vib.* **333**(18), 4214–4231 (2014).
37. K.-C. Liu, P. Maghami, and C. Blaurock, "Reaction wheel disturbance modeling, jitter analysis, and validation tests for solar dynamics observatory," in *AIAA Guidance, Navig. Control Conf. and Exhibit*, pp. 1–18 (2008).
38. R. A. Masterson, D. W. Miller, and R. L. Grogan, "Development and validation of reaction wheel disturbance models: empirical model," *J. Sound Vib.* **249**(3), 575–598 (2002).
39. B. Gerlach and M. E. R. Seiler, "Low noise five-axis magnetic bearing reaction wheel," in *IFAC Proc. Vol. (IFAC-PapersOnline)*, vol. 4, pp. 572–577 (2006).
40. J. I. Thorpe, C. Parvini, and J. Trigo-Rodriguez, "Detection and characterization of micrometeoroids with LISA pathfinder," *Astron. Astrophys.* **107**, 1–6 (2015).
41. E. Kramer et al., "Material selection for cryogenic support structures," *J. Low Temp. Phys.* **176**(5–6), 1103–1108 (2014).
42. M. B. Levine and C. White, "Material damping experiments at cryogenic temperatures," *Proc. SPIE* **5179**, 165 (2003).
43. J. Hinkle et al., "Submicron friction mechanics at ambient and cryogenic temperatures," *Proc. SPIE* **5899**, 589910 (2005).
44. L. D. Peterson and J. D. Hinkle, "What limits the achievable areal densities of large aperture space telescopes?" *Proc. SPIE* **5899**, 58990A (2005).
45. S. Fransen, D. Doyle, and B. Catanzaro, "Opto-mechanical modeling of the Herschel Space Telescope at ESA/ESTEC," *Proc. SPIE* **8336**, 833604 (2011).

46. B. E. Catanzaro et al., "UltraLITE glass/composite hybrid mirror," *Proc. SPIE* **4013** (2000).
47. L. Feinberg et al., "Space telescope design considerations," *Opt. Eng.* **51**(1), 011006 (2012).
48. A. Elgafy, O. Mesalhy, and K. Lafdi, "Numerical and experimental investigations of melting and solidification processes of high melting point PCM in a cylindrical enclosure," *J. Heat Transfer* **126**(5), 869–875 (2004).
49. C. I. Foster et al., "The solar array-induced disturbance of the Hubble Space Telescope Pointing System," Technical Report NASA-TP-3556, M-782, NAS 1.60:3556 NASA (1995).
50. E. A. Thornton and Y. A. Kim, "Thermally induced bending vibrations of a flexible rolled-up solar array," in *34th Struct., Struct. Dyn. and Mater. Conf.* (1993).
51. B. A. Boley, "Survey of recent developments in the fields of heat conduction in solids and thermo-elasticity," *Nucl. Eng. Des.* **18**(3), 377–399 (1972).
52. R. Kawamura et al., "Fundamental thermo-elasticity equations for thermally induced flexural vibration problems for inhomogeneous plates and thermo-elastic dynamical responses to a sinusoidally varying surface temperature," *J. Eng. Math.* **61**(2–4), 143–160 (2008).
53. P. Malik and R. Kadoli, "Thermal induced motion of functionally graded beams subjected to surface heating," *Ain Shams Eng. J.* **9**(1), 149–160 (2018).
54. S. M. Alipour, Y. Kiani, and M. R. Eslami, "Rapid heating of FGM rectangular plates," *Acta Mech.* **227**(2), 421–436 (2016).
55. Y. A. Kim, "Thermal creak induced dynamics of space structures," PhD thesis, Massachusetts Institute of Technology (1998).
56. L. C. Hale and A. H. Slocum, "Optimal design techniques for kinematic couplings," *Precis. Eng.* **25**(2), 114–127 (2001).
57. E. M. Wolf et al., "JWST mirror and actuator performance at cryo-vacuum," *Proc. SPIE* **10698**, 1069808 (2018).
58. J. Arenberg et al., "Status of the JWST sunshield and spacecraft," *Proc. SPIE* **9904**, 990405 (2016).
59. J. M. Howard, "Optical modeling activities for the James Webb Space Telescope (JWST) project: I. The linear optical model," *Proc. SPIE* **5178** (2004).
60. J. M. Howard, "Optical modeling activities for NASA's James Webb Space Telescope (JWST): III. Wavefront aberrations due to alignment and figure compensation," *Proc. SPIE* **6675**, 667503 (2007).
61. J. M. Howard, "Optical modeling activities for NASA's James Webb Space Telescope (JWST): IV. Overview and introduction of MATLAB based toolkits used to interface with optical design software," *Proc. SPIE* **6668**, 666804 (2007).
62. J. M. Howard and L. D. Feinberg, "Optical modeling activities for NASA's James Webb Space Telescope (JWST): VI. Secondary mirror figure compensation using primary mirror segment motions," *Proc. SPIE* **7436**, 74360C (2009).
63. J. M. Howard and K. Ha, "Optical modeling activities for the James Webb Space Telescope (JWST) project: II. Determining image motion and wavefront error over an extended field of view with a segmented optical system," *Proc. SPIE* **5487** (2004).
64. J. M. Howard et al., "Optical modeling activities for NASA's James Webb Space Telescope (JWST): Part V. Operational alignment updates," *Proc. SPIE* **7017**, 70170X (2008).
65. J. D. Johnston et al., "Integrated modeling activities for the James Webb Space Telescope: structural-thermal-optical analysis," *Proc. SPIE* **5487**, 588 (2004).
66. J. M. Howard, "Optical integrated modeling activities for the James Webb Space Telescope (JWST)," *Proc. SPIE* **8336**, 83360E (2011).
67. H. P. Stahl, L. D. Feinberg, and S. C. Texter, "JWST primary mirror material selection," *Proc. SPIE* **5487**, 818 (2004).
68. P. A. Lightsey et al., "James Webb Space Telescope: large deployable cryogenic telescope in space," *Opt. Eng.* **51**(1), 011003 (2012).
69. P. Reynolds, C. Atkinson, and L. Gliman, "Design and development of the primary and secondary mirror deployment systems of the cryogenic JWST," in *37th Aerosp. Mech. Symp.*, pp 29–44 (2004).

70. R. M. Warden, "Cryogenic nano-actuator for JWST," in *38th Aerosp. Mech. Symp.* (2006).
71. J. Scott Knight et al., "Observatory alignment of the James Webb Space Telescope," *Proc. SPIE* **8442**, 84422C (2012).
72. D. D. Waldie and L. N. Gilman, "Technology development for large deployable sunshield to achieve cryogenic environment," in *AIAA Space 2004 Conf. and Expo.*, San Diego, Vol. 2, pp. 1396–1405 (2004).
73. M. R. Bolcar et al., "Technology gap assessment for a future large-aperture ultraviolet-optical-infrared space telescope," *J. Astron. Telesc. Instrum. Syst.* **2**(4), 041209 (2016).
74. D. Redding et al., "HabEx Lite: a starshade-only habitable exoplanet imager alternative," *Proc. SPIE* **10698**, 106980X (2018).
75. Origins Space Telescope Study Team, "Mission concept study report," https://asd.gsfc.nasa.gov/firs/docs/OriginsVolume1MissionConceptStudyReport.pdf (2019).
76. T. Tupper Hyde and M. Postman, "Technology development plan for the Advanced Technology Large Aperture Space Telescope (ATLAST): a roadmap for UVIOR technology, 2010-2020," Technical Report, NASA Goddard Space Flight Centre (2010).
77. LUVOIR TEAM. "LUVOIR final report," Technical Report, NASA (2019).
78. LUVOIR Team, "LUVOIR interim report," Technical Report, NASA (2018).
79. J. W. Arenberg et al., "LUVOIR thermal architecture," *Proc. SPIE* **10698**, 1069814 (2018).
80. M. J. Eisenhower et al., "ATLAST ULE mirror segment performance analytical predictions based on thermally induced distortions," *Proc. SPIE* **9602**, 96020A (2015).
81. T. Segert et al., "Dobson space telescope: development of an optical payload of the next generation," *Proc. SPIE* **10567**, 105673E (2006).
82. T. Segert, B. Danziger, and M. Lieder, "Dobson space telescope the future of Microsat based observation," Technical Report, DLR, Berlin.
83. EOPortal, "Dobson space telescope," https://directory.eoportal.org/web/eoportal/satellite-missions/content/-/article/dobson-2.
84. E. Agasid, K. Ennico-Smith, and A. Rademacher, "Collapsible Space Telescope (CST) for nanosatellite imaging and observation," in *Proc. 27th Annu. AIAA/USU Conf. Small Satell.* pp. 1–5 (2013).
85. M. Komatsu and S. Nakasuka, "University of Tokyo Nano Satellite Project 'PRISM'," *Trans. JSASS Space Technol. Jpn.* **7**, 19–24 (2008).
86. Y. Sato et al., "Extensible flexible optical system for nano-scale remote sensing satellite "PRISM"," *Trans. JSASS Space Technol. Jpn.* **7**, 13–18 (2008).
87. T. Inamori et al., "Attitude stabilization for the nano remote sensing satellite PRISM," *J. Aerosp. Eng.* **26**(3), 594–602 (2013).
88. P. Hallibert and A. Z. Marchi, "Developments in active optics for space instruments: an ESA perspective," *Proc. SPIE* **9912**, 99121H (2016).
89. F. Simonetti et al., "Large aperture telescope for advanced Lidar system," *Opt. Eng.* **49**(7), 073001 (2010).
90. A. Z. Marchi et al., "Technological developments for ultra-lightweight, large aperture, deployable mirror for space telescopes," *Proc. SPIE* **10565**, 105651X (2017).
91. S. J. Thompson et al., "Large aperture telescope technology: a design for an active light-weight multi-segmented fold-out space mirror," *Proc. SPIE* **10565**, 105651Y (2010).
92. P. Mazzinghi et al., "An ultra-lightweight, large aperture, deployable telescope for advanced Lidar applications," *Proc. SPIE* **10567**, 105670E (2006).
93. J. Champagne et al., "CubeSat image resolution capabilities with deployable optics and current imaging technology," in *28th Annu. AIAA/USU Conf. Small Satell.* (2014).
94. D. Farrah et al., "Review: far-infrared instrumentation and technology development for the next decade," *J. Astron. Telesc. Instrum. Syst.* **5**(2), 020901 (2019).
95. N. Schwartz et al., "A segmented deployable primary mirror for earth observation from a CubeSat platform," in *Proc. AIAA/USU Conf. Small Satell.*, vol. SSC16, p. SSC16–WK–23 (2016).
96. N. Schwartz et al., "Laboratory demonstration of an active optics system for high-resolution deployable CubeSat," in *4S Symp.*, vol. 1, pp. 1–15 (2018).
97. D. Dolkens et al., "Design and optimization of a deployable telescope for Earth observation," *Draft J. Pap.* (2019).

98. M. Corvers, "Design of the deployment mechanism for the primary mirror of a deployable space telescope," https://repository.tudelft.nl/islandora/object/uuid%3Aa8bbf4a1-1222-41e0-96f5-94aa33a93d45?collection=education (2018).
99. A. Krikken, "Design of the secondary mirror support structure for the deployable space telescope," https://repository.tudelft.nl/islandora/object/uuid%3A9252841c-7a7c-4c8c-a418-9127b724d364?collection=education (2018).
100. J. W. Lopes Barreto, "Deployable space telescope: optimal boom design for high precision deployment of the secondary mirror," https://repository.tudelft.nl/islandora/object/uuid%3Ad3d3be57-0136-4258-95b5-a97e70a9d167?collection=education (2017).
101. S. M. Pepper, "Design of a primary mirror fine positioning mechanism for a deployable space telescope," https://repository.tudelft.nl/islandora/object/uuid%3A5763b240-4f3e-42ba-bb20-aab6e97b1489?collection=education (2018).
102. M. Voorn, "Initiating the testing phase of a deployable space telescope: an experimental characterisation of hysteresis in CORE hinges," https://repository.tudelft.nl/islandora/object/uuid%3Ae552e4e7-e2fb-402e-9923-2954c2d8a01f?collection=education (2018).
103. D. Dolkens, H. Kuiper, and V. V. Corbacho, "The deployable telescope: a cutting-edge solution for high spatial and temporal resolved Earth observation," *Adv. Opt. Technol.* **7**(6), 365–376 (2018).
104. M. S. Lake et al., "Experimental characterization of hysteresis in a revolute joint for precision deployable structures," in *38th AIAA Struct., Struct. Dyn., and Mater. Conf.*, Kissimmee, Florida, pp. 1–12 (1997).
105. M. S. Lake et al., "A deployable primary mirror for space telescopes," *Proc. SPIE* **3785** (1999).
106. J. D. Hinkle et al., "Technology for an Earth observing deployed Lidar telescope," in *48th AIAA/ASME/ASCE/AHS/ASC Struct., Struct. Dyn., and Mater. Conf.*, Honolulu (2007).
107. M. J. Silver et al., "Precision high strain composite hinges for the deployable in-space coherent imaging telescope," in *3rd AIAA Spacecr. Struct. Conf.*, pp. 1–21 (2016).
108. M. A. Echter et al., "Recent developments in precision high strain composite hinges for deployable space telescopes," in *AIAA Spacecr. Struct. Conf.*, p. 0939 (2018).
109. P. A. Warren, M. J. Silver, and B. J. Dobson, "Lightweight optical barrel assembly structures for large deployable space telescopes," *Proc. SPIE* **7436**, 74360B (2009).
110. P. A. Warren et al., "Experimental characterization of deployable outer barrel assemblies for large space telescopes," *Proc. SPIE* **8860**, 886008 (2013).
111. C. Underwood et al., "Using CubeSat/micro-satellite technology to demonstrate the Autonomous Assembly of a Reconfigurable Space Telescope (AAReST)," *Acta Astronaut.* **114**, 112–122 (2015).
112. C. Underwood et al., "AAReST Autonomous Assembly Reconfigurable Space Telescope flight demonstrator," in *69th Int. Astronaut. Congr.*, International Astronautical Federation, Bremen (2018).
113. J. Steeves et al., "Multilayer active shell mirrors for space telescopes," *Proc. SPIE* **9912**, 99121K (2016).
114. H. M. Y. C. Mallikarachchi and S. Pellegrino, "Design of ultrathin composite self-deployable booms," *J. Spacecr. Rockets* **51**(6), 1811–1821 (2014).
115. S. Huybrechts et al., "Structural design for deployable optical telescopes," in *IEEE Aerosp. Conf. Proc. (Cat. No. 00TH8484)*, IEEE (2000).
116. K. N. Schrader et al., "Integrated control system development for phasing and vibration suppression for a sparse-array telescope," *Proc. SPIE* **4849**, 134 (2002).
117. S. A. Lane et al., "Active vibration control of a deployable optical telescope," *J. Spacecr. Rockets* **45**(3), 568–586 (2008).
118. M. Powers et al., "Assessment of a large aperture telescope trade space and active opto-mechanical control architecture," (1997).
119. J. L. Domber et al., "Dimensional repeatability of an elastically folded composite hinge for deployed spacecraft optics," *J. Spacecr. Rockets* **39**(5), 646–652 (2002).
120. P. A. Lightsey et al., "Optical budgeting for LUVOIR," *Proc. SPIE* **10698**, 1069813 (2018).
121. M. S. Lake, L. D. Peterson, and M. B. Levine, "Rationale for defining structural requirements for large space telescopes," *J. Spacecr. Rockets* **39**(5), 674–681 (2002).

122. J.-W. Arink, "Thermal-mechanical design of a baffle for the deployable space telescope," https://repository.tudelft.nl/islandora/object/uuid%3A4ff37e5f-f155-44bb-8fee-408f6d799053?collection=education (2019).
123. T. van Wees, "Thermal modelling & analysis of the deployable space telescope," https://repository.tudelft.nl/islandora/object/uuid%3Af698fca7-205b-487d-b521-83d7f85e6fef?collection=education (2019).
124. D. Farhadi Machekposhti, N. Tolou, and J. L. Herder, "A review on compliant joints and rigid-body constant velocity universal joints toward the design of compliant Homokinetic couplings," *J. Mech. Des.* **137**(3), 032301 (2015).
125. M. East et al., "Material selection for far infrared telescope mirrors," *Proc. SPIE* **10698**, 106981N (2018).

Víctor Villalba, MSc, is a PhD candidate at the Department of Space Engineering of the Delft University of Technology. He holds a bachelor's degree in aerospace engineering from the University of Seville and an MSc in space science and technology from Cranfield University and the Lulea University of Technology. His research interest is in stable structures and actuation mechanisms for stabilization of deployable space telescopes.

Hans Kuiper is an assistant professor at the Department of Space Engineering, Delft University of Technology. Previously he held technical positions at the Dutch high-tech industry for more than 30 years. He holds an MSc in applied physics from the Eindhoven University of Technology and a PhD in space systems engineering from the Delft University of Technology. His research interest is in the systems engineering of spaceborne optical instruments.

Eberhard Gill is the chair of Space Systems Engineering at the Faculty of Aerospace Engineering at the Delft University of Technology and head of the Department of Space Engineering. His research interests comprise the guidance, navigation, and control of distributed and miniaturized space systems and its engineering. He holds a PhD in theoretical astrophysics from the University of Tübingen, Germany.